



The investigation of copper-based impregnated activated carbons prepared from water-soluble materials for broad spectrum respirator applications

J.W.H. Smith^a, P. Westreich^a, H. Abdellatif^a, P. Filbee-Dexter^a, A.J. Smith^a, T.E. Wood^b, L.M. Croll^c, J.H. Reynolds^c, J.R. Dahn^{a,d,*}

^a Department of Physics and Atmospheric Science, Dalhousie University, Halifax, Nova Scotia, B3H 3J5, Canada

^b 3M Company, St. Paul, MN, 55144, USA

^c 3M Canada Company, Brockville, Ontario, K6V 5V8, Canada

^d Department of Chemistry, Dalhousie University, Halifax, Nova Scotia, B3H 4J3, Canada

ARTICLE INFO

Article history:

Received 28 September 2009

Received in revised form 12 April 2010

Accepted 13 April 2010

Available online 18 April 2010

Keywords:

Impregnated activated carbon

Impregnant distribution

Nitric acid treatment

Gas filtration capacity

Relative stoichiometric ratio of reaction

ABSTRACT

The preparation of impregnated activated carbons (IACs) from aqueous, copper-containing solutions for broad spectrum gas filtration applications is studied here. Several samples were studied to determine the effect that impregnant loading, impregnant distribution and impregnant recipe had on the overall performance. Dynamic flow testing was used to determine the gas filtration capacity of the IAC samples versus a variety of challenge gases. X-ray diffraction (XRD), scanning electron microscopy (SEM) and energy dispersive X-ray analysis (EDX) were used to characterize the impregnant distribution on the carbon as a function of impregnant loading. Oven tests were performed to determine the thermal stability of the IAC samples exposed to elevated temperatures. The role impregnant distribution plays in gas filtration capacity and the overall performance of the IAC samples is discussed. The IAC samples prepared in this work were found to have gas filtration capacities as good as or better than broad spectrum respirator carbon samples prepared from the patent literature. IACs impregnated with an aqueous 2.4 M $\text{Cu}(\text{NO}_3)_2/0.04 \text{ M H}_3\text{PO}_4/12\text{MoO}_3/4 \text{ M HNO}_3$ solution that were heated to 200 °C under argon were found to have the best overall performance of the samples studied in this work.

© 2010 Elsevier B.V. All rights reserved.

1. Introduction

Adding properly selected impregnants to activated carbon (AC) has been proven to enhance their natural ability to filter certain irritating and toxic gases. Impregnated activated carbon (IAC) has the capability to filter gases that cannot be filtered by virgin activated carbon [1–7]. Individuals in high-risk professions such as first responders or military personnel may be deployed in situations where an unknown toxin is present in the air. For their protection and to expedite their ability to function in hazardous environments it is desirable to provide a gas mask capable of filtering a wide variety of irritating and toxic gases. Gas mask filters used in such broad spectrum filtration applications are usually filled with impregnated activated carbons. Historically, IACs used in broad spectrum applications have been prepared from impregnating solutions containing copper compounds [1,8]. These types of solutions usually rely on ammonia and ammonium salts to help

dissolve the copper-containing (and other metallic) impregnants and distribute them on the activated carbon surface [1,9]. Impregnating activated carbons with ammoniacal solutions produces a large amount of ammonia waste product (e.g. ammonia off-gassing during drying and/or excess ammoniacal impregnating solution). Ammonia is considered to be a toxic substance under section 64 of the Canadian Environmental Protection Act [10], therefore specialized equipment and treatment procedures are required to deal with the ammonia waste product. A broad spectrum impregnated activated carbon that can be produced without the use of ammoniacal solutions is therefore desirable from an economic and environmental standpoint.

A wide variety of IAC samples prepared from aqueous, copper-containing solutions were studied in this work. Samples were characterized using techniques such as X-ray diffraction (XRD), scanning electron microscopy (SEM), energy dispersive X-ray analysis (EDX) and thermal stability tests. Dynamic flow testing was performed on the IAC samples using sulfur dioxide (SO_2), ammonia (NH_3) and hydrogen cyanide (HCN) challenge gases. Treating the AC substrate with nitric acid (HNO_3) was found to improve impregnant distribution and increase gas filtration capacity. $\text{Cu}(\text{NO}_3)_2$, HNO_3 and phosphomolybdic acid ($\text{H}_3\text{PO}_4 \cdot 12\text{MoO}_3$) were combined to form an aqueous impregnating solution capable of impregnating

* Corresponding author at: Department of Physics and Atmospheric Science, Dalhousie University, Halifax, Nova Scotia, B3H 3J5, Canada. Tel.: +1 902 494 2991; fax: +1 902 494 5191.

E-mail address: jeff.dahn@dal.ca (J.R. Dahn).

the AC substrate in a simple and efficient manner. This impregnating solution and appropriate heat treatments produced IACs capable of filtering SO_2 , NH_3 and HCN gases at levels comparable to IAC samples prepared from ammoniacal impregnating solutions described in the literature [9]. The thermal stability of the IACs prepared in this study was compared to commercially available IAC samples using oven tests to simulate storage at elevated temperatures. IACs prepared in this work were found to be at least as thermally stable as a commercially available IAC.

2. Experimental details

2.1. Chemicals used

The chemicals used to prepare aqueous impregnating solutions were copper nitrate trihydrate ($\text{Cu}(\text{NO}_3)_2 \cdot 3\text{H}_2\text{O}$ (or equivalently copper nitrate hemi(pentahydrate) ($\text{Cu}(\text{NO}_3)_2 \cdot 2.5\text{H}_2\text{O}$)), Molybdophosphoric acid hydrate ($\text{H}_3\text{PO}_4 \cdot 12\text{MoO}_3 \cdot x\text{H}_2\text{O}$), copper sulfate pentahydrate ($\text{CuSO}_4 \cdot 5\text{H}_2\text{O}$), sodium molybdate dihydrate ($\text{Na}_2\text{MoO}_4 \cdot 2\text{H}_2\text{O}$) and nitric acid (HNO_3). These were dissolved, in various combinations, in distilled water. The chemicals were obtained from Alfa Aesar ($\text{Cu}(\text{NO}_3)_2 \cdot 2.5\text{H}_2\text{O}$, $\text{H}_3\text{PO}_4 \cdot 12\text{MoO}_3 \cdot x\text{H}_2\text{O}$ and $\text{CuSO}_4 \cdot 5\text{H}_2\text{O}$), J.T. Baker ($\text{Na}_2\text{MoO}_4 \cdot 2\text{H}_2\text{O}$) and Sigma–Aldrich (70% concentrated HNO_3) respectively and were of reagent grade.

The chemicals used to prepare ammoniacal impregnating solutions were basic copper carbonate ($\text{Cu}_2\text{CO}_3(\text{OH})_2$), ammonium carbonate ($(\text{NH}_4)_2\text{CO}_3$), ammonium molybdate ($(\text{NH}_4)_2\text{Mo}_2\text{O}_7$) and ammonium sulfate ($(\text{NH}_4)_2\text{SO}_4$). These materials were dissolved in an approximately 0.85:1 ammonium hydroxide and distilled water solution. These chemicals were obtained from Sigma–Aldrich, 3 M Canada, Johnson Matthey Catalog Company and Sigma respectively, and are of reagent grade. The NH_4OH solution was obtained from Sigma–Aldrich (28–30% concentration).

2.2. Sample preparation

IAC samples were prepared using Kuraray GC, a granular activated carbon commercially available from Kuraray Chemical Co. (Osaka, Japan). This activated carbon is derived from coconut shells and has been acid-washed to lower the ash content (0.4%, w/w). Kuraray GC (referred to subsequently as GC) has a particle mesh size of 12×35 , which corresponds to a granule size of approximately 1.70–0.50 mm. Further characterizations of GC have been performed in previous work and are published in the literature [11,12]. IAC samples were prepared on virgin GC and GC that had been pre-treated with HNO_3 . Two different HNO_3 treatments were employed, boiling GC in 5 M HNO_3 and imbibing GC with HNO_3 of different concentrations. The details of boiling GC in 5 M HNO_3 have been published in the literature [11,12]. GC that was boiled in 5 M HNO_3 will be denoted A-GC in the ensuing discussions.

IAC samples were prepared from several different types of impregnating solutions. Aqueous solutions of $\text{Cu}(\text{NO}_3)_2$ varying in concentration from 1.7 M to 2.4 M were added to GC and A-GC in the simplest cases. An aqueous solution containing 1.3 M $\text{Cu}(\text{NO}_3)_2$ and 0.3 M CuSO_4 was used in combination with a 0.4 M Na_2MoO_4 solution to impregnate A-GC in multiple imbibing and drying steps. IAC samples were also prepared from aqueous solutions composed of $\text{Cu}(\text{NO}_3)_2$, $\text{H}_3\text{PO}_4 \cdot 12\text{MoO}_3$ and HNO_3 in varying concentrations. The concentration of the $\text{Cu}(\text{NO}_3)_2$ present in these solutions varied from approximately 1.6 M to 2.4 M. The $\text{H}_3\text{PO}_4 \cdot 12\text{MoO}_3$ concentrations ranged from 0.02 M to 0.04 M and the HNO_3 concentration ranged from 1 M to 5 M. The AC substrate was impregnated using the imbibing method (also known as the incipient wetness method) which has been described in the literature [5,11].

All of the IAC samples prepared from these types of solutions were dried in an inert argon atmosphere to a maximum final drying temperature, T_F , ranging from 190 °C to 220 °C. The elevated drying temperatures were used to decompose the $\text{Cu}(\text{NO}_3)_2$ impregnant to CuO . Typically the IAC samples were placed in a tube furnace under an argon gas flow of roughly 60 mL/min for 20–30 min prior to heating. The samples were then heated to the maximum final drying temperature, and held for a minimum of 2 h. The IACs were allowed to cool under the argon gas flow before being removed from the tube furnace.

For comparison, IAC samples were prepared according to the ‘preferred’ impregnating solution described in the literature [9]. This ammoniacal solution was prepared by combining desired amounts of basic copper carbonate ($\text{Cu}_2\text{CO}_3(\text{OH})_2$), ammonium carbonate ($(\text{NH}_4)_2\text{CO}_3$), ammonium molybdate ($(\text{NH}_4)_2\text{Mo}_2\text{O}_7$) and ammonium sulfate ($(\text{NH}_4)_2\text{SO}_4$) with an approximately 0.85:1 ammonium hydroxide and distilled water solution. The chemicals were added to a 100 ml Nalgene bottle and the NH_4OH and distilled water were then added. The contents were then stirred until fully dissolved. IAC samples were prepared in two imbibing and drying steps, following the procedure outlined in [9]. The samples were dried, in air, to $T_F = 180$ °C.

The overall impregnant loading on the IAC samples was determined by gravimetric analysis and is expressed as the percent of impregnant loading by weight (% load (wt)). The relative uncertainty of the overall impregnant loading on the samples is 2%. Impregnant loading that is expressed in mmol impregnant/g GC was estimated from the volume and concentration of impregnating solution added to the virgin GC. The relative uncertainty is 0.1 mmol impregnant/g GC.

2.3. Sample characterization

X-ray diffraction was performed using a Rigaku MiniFlex X-ray diffractometer at a scan rate of 0.05°/step and a dwell time of 30 s/step. This diffractometer uses variable slits to keep the size of the X-ray beam on the sample constant as the scattering angle is changed. A Phillips diffractometer was also used to conduct powder XRD experiments. This diffractometer uses fixed slits. Typical scan conditions used for the Phillips diffractometer were 0.05°/step with a dwell time of 6 s per step. Prior to analysis all samples were ground to a powder using a mortar and pestle.

A Hitachi S-4700 field emission SEM equipped with energy dispersive X-ray analysis was used to image IAC samples. Typical conditions employed during imaging were a working distance of 12 mm, an accelerating voltage of 20 kV and a beam extraction current of 15 μA . In order to image the inner pores of the impregnated activated carbon (IAC), granules were cut with a scalpel and mounted on a SEM stub. The granules were imbedded in a conducting carbon paste to ensure stability and facilitate imaging.

Thermal stability experiments were conducted on IAC samples placed within a VWR Scientific gravity convection oven. Experimental details and a description of the sample holder are given in the literature [13]. The filled sample holder was placed in a pre-heated oven (in air) through an access hole at the top of the oven. The temperature of the sample was monitored as a function of time at the core and on the surface by two K-type thermocouples [14]. A third K-type thermocouple, imbedded in a brass block, was used to measure the temperature inside the oven. Data from the thermocouples was recorded by a computer that was controlled by DAS-Wizard software.

2.4. Dynamic flow testing

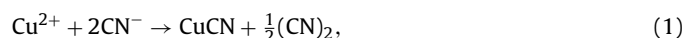
On-carbon samples were tested for filtration capacity using sulfur dioxide (SO_2), ammonia (NH_3) and hydrogen cyanide (HCN)

Table 1

Detailed description of IAC samples studied in this work and the contents of the impregnating solutions they were prepared from. Samples marked with an asterisk were prepared in multiple imbibing and drying cycles.

Sample name	% Load (wt)	Base carbon	Impregnating solution contents	Detailed impregnant load (mmol/g AC)
N1	30*	GC	2.90 g (NH ₄) ₂ CO ₃ + 0.91 g (NH ₄) ₂ MoO ₇ + 5.07 g Cu ₂ CO ₃ (OH) ₂ + 1.22 g (NH ₄) ₂ SO ₄ dissolved in solution containing 9.9 mL NH ₄ OH + 11.6 mL distilled water	2.3 Cu + 0.3 Mo
W1	15	GC	2.3 M Cu(NO ₃) ₂	1.9 Cu
W2	13	A-GC	2.3 M Cu(NO ₃) ₂	1.9 Cu
W3	31*	GC	(i) 1.3 M Cu(NO ₃) ₂ /0.3 M CuSO ₄ (ii) 0.4 M Na ₂ MoO ₄	2.5 Cu + 0.3 Mo
W4	30*	A-GC	(i) 1.3 M Cu(NO ₃) ₂ /0.3 M CuSO ₄ (ii) 0.4 M Na ₂ MoO ₄	2.5 Cu + 0.3 Mo
W5	13*	GC	1.7 M Cu(NO ₃) ₂ /0.02 M H ₃ PO ₄ ·12MoO ₃ /5 M HNO ₃	1.4 Cu + 0.2 Mo
W6	13*	GC	1.7 M Cu(NO ₃) ₂ /0.02 M H ₃ PO ₄ ·12MoO ₃ /2.5 M HNO ₃	1.4 Cu + 0.2 Mo
W7	13*	GC	1.7 M Cu(NO ₃) ₂ /0.02 M H ₃ PO ₄ ·12MoO ₃ /1 M HNO ₃	1.4 Cu + 0.2 Mo
W8	15	GC	1.6 M Cu(NO ₃) ₂ /0.02 M H ₃ PO ₄ ·12MoO ₃ /4 M HNO ₃	1.3 Cu + 0.2 Mo
W9	20	GC	2.4 M Cu(NO ₃) ₂ /0.04 M H ₃ PO ₄ ·12MoO ₃ /4 M HNO ₃	1.9 Cu + 0.4 Mo
W10	22*	GC	1.7 M Cu(NO ₃) ₂ /0.04 M H ₃ PO ₄ ·12MoO ₃ /1.2 M HNO ₃	1.9 Cu + 0.4 Mo
W11	19	GC	3.3 M Cu(NO ₃) ₂	2.3 Cu

challenge gases. The SO₂ and NH₃ tests were performed at Dalhousie University. Due to its acutely toxic nature (an exposure of 300 ppm can be fatal in minutes) [15], the HCN testing was performed at 3 M Canada, which is properly equipped to handle such gases. Samples with a 0.75 g mass of base carbon (the actual sample mass was greater than 0.75 g due to the mass of the impregnant) were tested. The IAC sample was exposed to 1000 ± 50 ppm challenge gas (SO₂ or NH₃) at an overall flow rate of 200 ± 5 mL/min for tests done at Dalhousie University. The effluent gas stream was bubbled into a scrubbing solution and the breakthrough of the challenge gas was determined by monitoring the pH of the scrubbing solution. The breakthrough time was chosen as the time when 36 ppm SO₂ (or 3.6 ppm NH₃) was detected in the scrubbing solution. Breakthrough times reported for SO₂ and NH₃ tests are an average of 2–4 measurements for each sample. Detailed descriptions of the testing apparatus and methods used at Dalhousie University have been published in the literature [5,6,11]. IAC samples tested for HCN filtration capacity at 3 M Canada were exposed to approximately 2000 ppm HCN gas at an overall flow rate of approximately 260 mL/min. The breakthrough time for HCN was chosen as the time when 5 ppm HCN concentration was detected. Due to the well documented reaction of copper (2+) with HCN [16]:



the effluent gas stream from the HCN tested samples must also be monitored for the presence of cyanogen ((CN)₂). A gas chromatograph with a flame ionization detector was used for both HCN and (CN)₂ detection. Only a single test for each sample was performed.

3. Results and discussion

Details of the IAC samples prepared in this study are listed in Table 1. The overall impregnant loading (% load (wt)), contents of the impregnating solution, detailed impregnant loading (mmol/g AC) and type of base carbon (GC or A-GC) are listed for reference. Samples that begin with “N” were prepared in NH₃-containing solutions and samples that begin with “W” were prepared in water-based, ammonia-free solutions. It should be noted that samples W5–W7 were prepared in two imbibing steps, first with HNO₃, then with the aqueous Cu(NO₃)₂ and H₃PO₄·12MoO₃ solution. Samples prepared in this manner did not appear to differ from IAC samples prepared in a single imbibing step (such as sample W8), therefore no distinction will be made between IAC samples prepared in one or two imbibing steps from aqueous solutions containing Cu(NO₃)₂ and H₃PO₄·12MoO₃ and HNO₃.

3.1. The effects of HNO₃ treatments

IAC samples prepared in this study were characterized using a variety of experimental techniques to determine the phase of the impregnant present after drying and how it was distributed on the AC substrate. Fig. 1 shows X-ray diffraction patterns obtained from IAC samples W1, W2 and N1 in panels (a), (b) and (c), respectively. For reference, the Bragg peak positions have been indicated using known values from [17].

Fig. 1(a) shows that the XRD pattern of sample W1 has pronounced diffraction peaks associated with a CuO impregnant phase, especially for the peaks located at 2θ values of approximately 35° and 38°. These intense, well defined peaks are indicative of relatively large grain-size CuO impregnant as can be inferred using the Scherrer equation [18]. The average grain size of the CuO impreg-

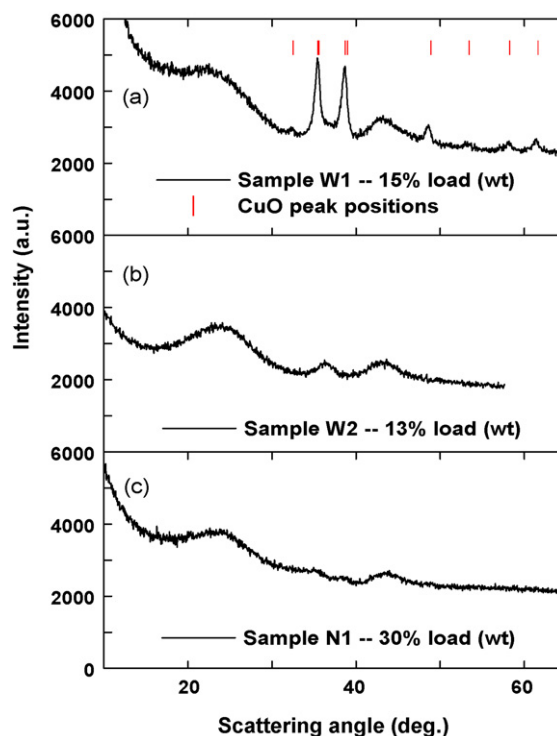


Fig. 1. X-ray diffraction patterns obtained from IAC samples W1, W2 and N1 are shown in panels (a), (b) and (c), respectively.

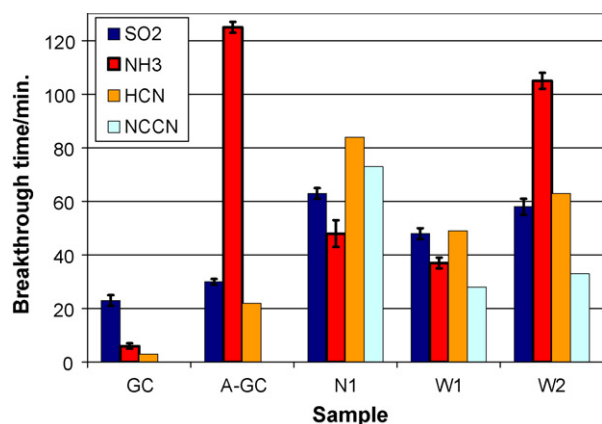


Fig. 2. Dynamic flow test results obtained for IAC samples W1, W2 and N1 versus SO₂, NH₃ and HCN challenge gases. Results obtained from testing virgin GC and A-GC are included for reference. The results obtained from SO₂ and NH₃ testing are averaged from 2–4 tests per sample, the error bars denote the deviation from the averaged value. Reported HCN and NCCN breakthrough times were obtained from a single flow test per sample.

nant for sample W1 was calculated using data from the two main diffraction peaks and was found to be 12 ± 1 nm. Fig. 1(b) shows that the diffraction pattern obtained from sample W2 has a single broad, low-intensity impregnant-related diffraction peak. This is indicative of relatively small grain-sized impregnant. The calculated average impregnant grain size for sample W2 was 5 ± 1 nm. The reduction in impregnant grain-size observed in sample W2 compared to W1 can be attributed to the HNO₃ treatment of the base carbon. It has been shown in the literature that treating AC with HNO₃ can improve its ability to adsorb aqueous metal ions [12,19]. The XRD pattern obtained from IAC sample N1 is shown in Fig. 1(c). This diffraction pattern shows broad, low-intensity CuO peaks indicative of small grain-sized impregnant. A heat-treated impregnated carbon sample showing a sharp diffraction pattern from the impregnant phase must have relatively large impregnant grains, indicative of a situation where the impregnant is not dispersed as a thin, even layer across the surfaces of the activated carbon. By contrast, an IAC with the same impregnant, the same loading and heated to the same temperature, showing only weak broad diffraction peaks from the impregnant phase, must have better distribution of the impregnant phase as it is comprised of relatively small sized grains, presumably well-spread on the AC surface. Thus, XRD experiments can shed light on the dispersion of the impregnant phase.

Well-dispersed impregnant distributed evenly on the activated carbon substrate has been shown to increase the stoichiometric ratio of reaction (SRR) between the impregnant and challenge gas [5,6,11]. We have shown a relationship between increasing impregnant grain size and decreasing SRR in previous work [20]. To determine the effect that impregnant distribution had on IAC samples W1, W2 and N1, dynamic flow testing was performed using SO₂, NH₃ and HCN challenge gases. The results of these tests are shown in Fig. 2. For comparison, flow test results obtained from virgin GC and A-GC samples are shown.

Comparison of the SO₂ and NH₃ flow test results shown in Fig. 2 demonstrates the effect of HNO₃ treatment on gas filtration capacity. Sample W2 displays a modest improvement in SO₂ capacity relative to W1. XRD patterns obtained from this sample indicated that it had smaller grain-size impregnant, and presumably better impregnant distribution, than sample W1 as was shown in Fig. 1(a) and (b).

Comparison of NH₃ flow test results for the GC, A-GC, W1 and W2 samples shows that the HNO₃ treatment dramatically increased NH₃ filtration capacity. HNO₃ treatments of GC carbon

have been shown to introduce acidic groups on the carbon surface [12] and the presence of these acidic groups is most likely responsible for the high NH₃ filtration capacity observed for the A-GC and W2 samples. Interactions between NH₃ gas and HNO₃ treated activated carbons have been discussed in the literature [21]. Work to better understand the interactions between NH₃ gas and the HNO₃ treated IACs discussed here is ongoing and will be reported in future work.

Comparison of the HCN flow test results in Fig. 2 indicates that the amount of Cu²⁺ impregnant present and the way it is dispersed on the AC substrate have a dramatic effect on filtration capacity. The Cu-species loadings listed in Table 1 show that samples W1 and W2 have 1.9 mmol Cu²⁺/g GC, whereas sample N1 has 2.3 mmol Cu²⁺/g GC. This can partly explain why sample N1 has higher HCN filtration capacity, as is shown in Fig. 2, however it does not fully explain the discrepancy. Comparison of the Cu²⁺ impregnant loading to the breakthrough time achieved shows that samples N1 and W2 are more efficient at filtering HCN than sample W1. Fig. 1(a)–(c) indicates that samples N1 and W2 have smaller grain-size impregnant, and presumably better impregnant distribution, than sample W1, so it is therefore reasonable to conclude that the smaller grain-sized impregnant results in increased HCN filtration capacity. Fig. 2 also shows that A-GC has longer breakthrough times than virgin GC when challenged with HCN gas. Research to understand the role that the HNO₃ treatment plays in HCN filtration for unimpregnated activated carbons is being conducted and will be reported in future work.

Equation 1 shows that NCCN gas is generated when Cu²⁺ impregnant is exposed to HCN gas. This reaction is discussed in the literature [16]. The breakthrough times reported for NCCN in Fig. 2 show that sample W1 has relatively little ability to retain the NCCN gas. It is known that when Cu²⁺ is used to filter HCN, additional materials containing chromium, molybdenum or tungsten must be added to capture the NCCN gas [1,9,16,22]. In order to address the poor NCCN capacity of the aqueous Cu(NO₃)₂ containing samples,

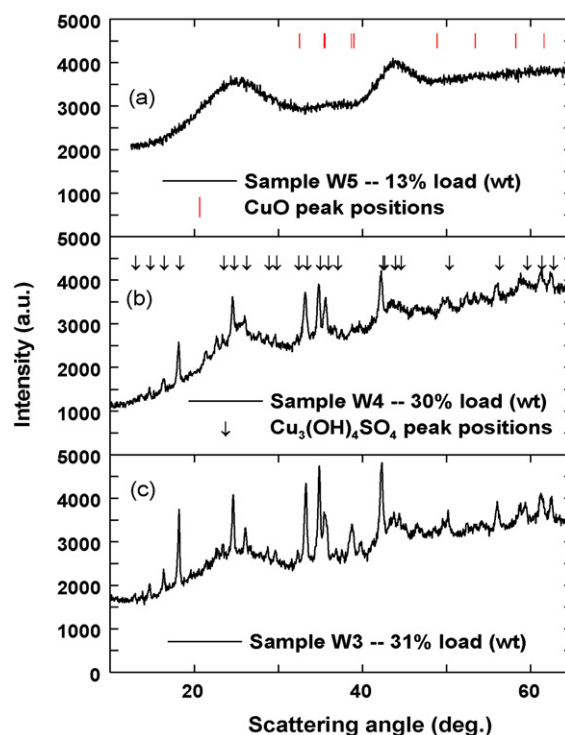


Fig. 3. XRD patterns obtained from IAC samples W5, W4 and W3 are shown in panels (a), (b) and (c), respectively. The main Bragg peak positions for CuO and antlerite (Cu₃(OH)₄SO₄) are shown for reference.

a study was conducted to find a suitable water-soluble impregnant to control the generation of NCCN.

3.2. Broad spectrum IAC study

On- and off-carbon studies were performed to identify a water-soluble impregnant(s) that could be combined with $\text{Cu}(\text{NO}_3)_2$ to prepare IAC samples capable of filtering SO_2 , NH_3 and HCN gases concurrently without releasing toxic NCCN gas. IAC samples W3, W4 and W5, listed in Table 1, were comparatively studied to determine their suitability for broad spectrum respirator applications. XRD patterns were obtained from IAC samples W5, W4 and W3 using a Rigaku Miniflex diffractometer and they are shown in

Figs. 3(a)–(c), respectively. The main Bragg peak positions for CuO and antlerite ($\text{Cu}_3(\text{OH})_4\text{SO}_4$) are shown for reference.

Fig. 3(b) and (c) shows that the dominant impregnant phase present after drying samples W3 and W4 was $\text{Cu}_3(\text{OH})_4\text{SO}_4$. Comparison of these figures show that sample W4 has less intense impregnant-related diffraction peaks, which indicates that the HNO_3 treatment may have helped improve impregnant distribution on this sample, however impregnant distribution on W4 was still considered poor. Fig. 3(a) shows that the X-ray diffraction pattern obtained from IAC sample W5 is virtually free of impregnant-related diffraction peaks, which is consistent with the presence of HNO_3 in the impregnating solution improving impregnant distribution. It should be observed that sample W5 has much

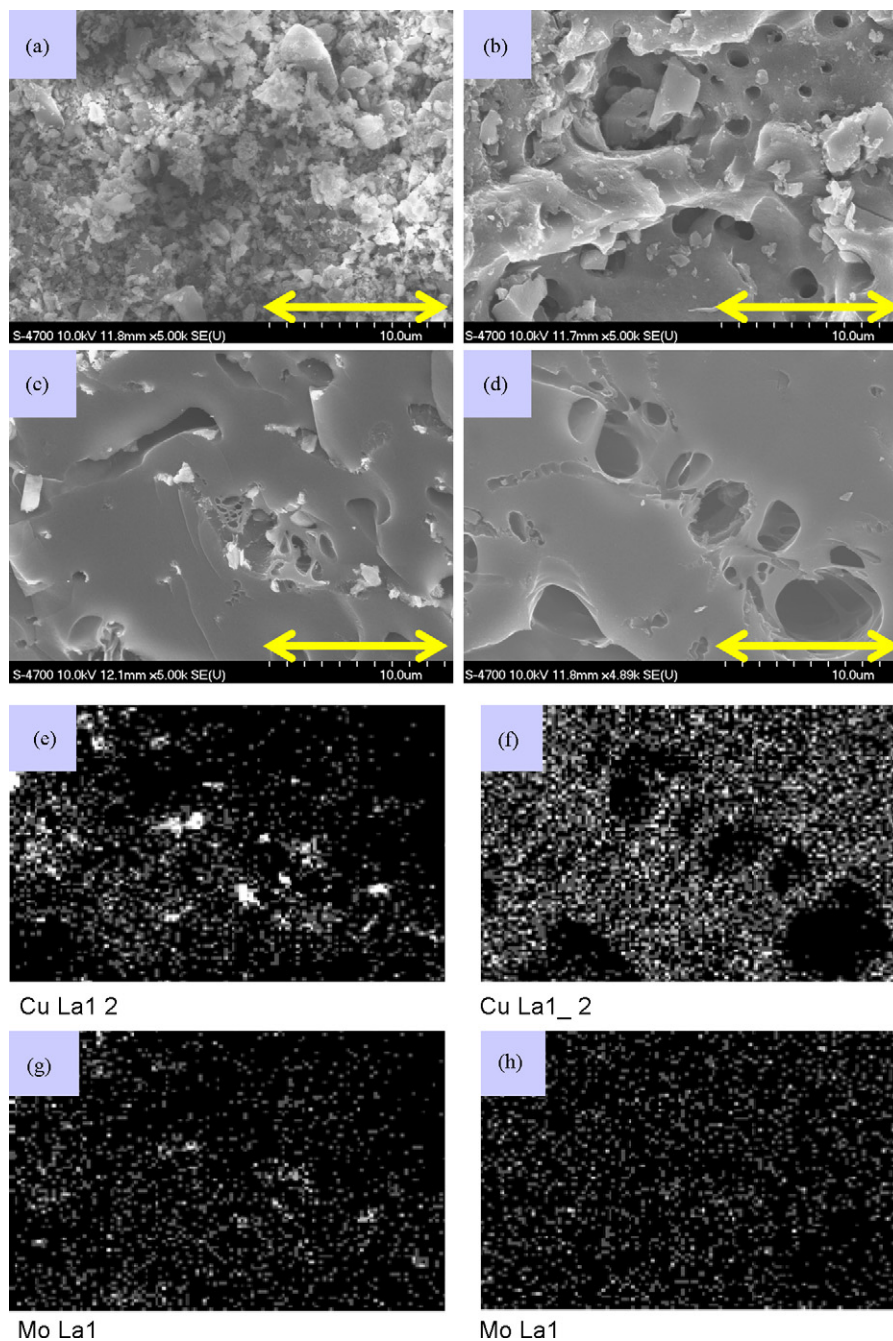


Fig. 4. Panels (a) and (c) show the outer surface and inner pore structure of a granule of carbon obtained from sample W3. Panels (b) and (d) show the outer surface and inner pore structure respectively of a granule of carbon obtained from sample W5. Panels (e) and (g) show Cu and Mo EDX distribution maps respectively of the area shown in panel (c). Panels (f) and (h) show Cu and Mo EDX distribution maps respectively of the area shown in panel (d). The white pixels in the EDX maps indicated the presence of the impregnant species (either Cu or Mo). The arrows shown in panels (a)–(d) represent a distance of 10 μm .

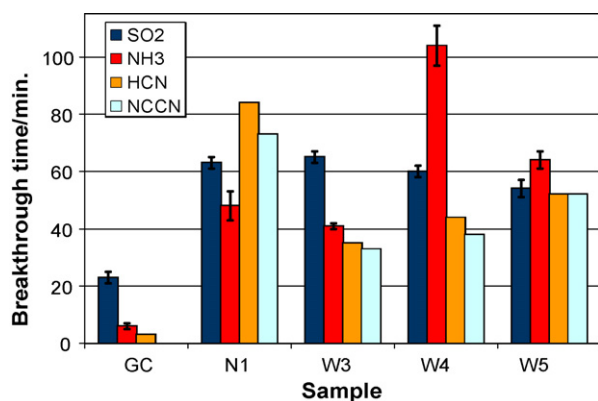


Fig. 5. Results obtained from challenging IAC samples W3, W4 and W5 with SO₂, NH₃ and HCN challenge gases. For comparison, flow test results obtained from virgin GC and sample N1 are shown. The values reported for SO₂ and NH₃ flow tests are average values obtained from 2 to 4 tests per sample. The error bars denote the deviation from the average value. The HCN and NCCN breakthrough times were obtained from a single flow test per sample.

lower overall impregnant loading than samples W3 and W4. IAC samples similar to W5, with higher impregnant loading, will be discussed in later sections.

To further study impregnant distribution, IAC samples W3 and W5 were characterized using SEM and EDX analysis, as is shown in Fig. 4. Panels (a) and (c) show the outer surface and inner pore structure of a granule of carbon obtained from sample W3. Panels (b) and (d) show the outer surface and inner pore structure respectively of a granule of carbon obtained from sample W5. Panels e and g show Cu and Mo EDX distribution maps respectively of the area shown in panel (c). Panels (f) and (h) show Cu and Mo EDX distribution maps respectively of the area shown in panel (d). The white pixels in the EDX maps indicate the presence of the impregnant species (either Cu or Mo). The arrows shown in panels (a)–(d) represent a distance of 10 μm.

Fig. 4(a) and (c) shows that IAC sample W3 has poor impregnant distribution. The SEM image shows the outer surface (Fig. 4(a)) is heavily covered by the impregnating materials, as was confirmed by EDX analysis (not shown). The inner pore structure, shown in Fig. 4(c), has “visual” signs of impregnant agglomeration. The EDX pixel maps shown in Fig. 4(e) and (g) confirm that these agglomerations are rich in the impregnating elements (Cu and Mo). Fig. 4(e) shows that the Cu-impregnant species is poorly distributed across the AC substrate, with most of the impregnant appearing in the agglomerations. By contrast, SEM images of sample W5 do not show any “visual” signs of impregnant(s) on the exterior or interior surfaces as can be seen in Fig. 4(b) and (d), respectively. The EDX pixel map shown in Fig. 4(f) is indicative of even Cu-impregnant distribution across the AC substrate. The EDX map of Mo-impregnant distribution shown in Fig. 4(h) indicates that the Mo and Cu impregnants are in intimate contact across the entire AC substrate. This intimate contact is believed to be an important factor in achieving well balanced HCN and NCCN filtration times and will be discussed in terms of dynamic flow test results.

Results obtained from IAC samples W3, W4 and W5 with SO₂, NH₃ and HCN challenge gases are reported in Fig. 5. For comparison, flow test results obtained from virgin GC and sample N1 are shown. Comparison of the flow test results in Fig. 5 for IAC samples W3 and W4 show that the HNO₃ treatment of the base carbon improved gas filtration capacity. Sample W4 has approximately the same SO₂ capacity as W3, but has longer HCN, NCCN and NH₃ breakthrough times. The importance of impregnant distribution is best illustrated by comparing the HCN flow test results reported in Fig. 5. Samples N1, W3 and W4 have approximately the same impregnant loading (as can be seen in Table 1), however sample N1 has much

Table 2

Combinations of aqueous solutions (reactants) and the proposed precipitation products (if any).

Reactants	Precipitation products
8 ml 3 M Cu(NO ₃) ₂ (aq) + 4 ml 0.4 M Na ₂ MoO ₄ (aq)	2 NaNO ₃ (aq) + CuMoO ₄ (s)
8 ml 3 M Cu(NO ₃) ₂ (aq) + 4 ml 0.1 M (NH ₄) ₂ Mo ₂ O ₇ (aq)	2 NH ₄ NO ₃ (aq) + CuMo ₂ O ₇ (s)
8 ml 0.6 M CuSO ₄ (aq) + 4 ml 0.4 M Na ₂ MoO ₄ (aq)	Na ₂ SO ₄ (aq) + CuMoO ₄ (s)
8 ml 0.6 M CuSO ₄ (aq) + 4 ml 0.1 M (NH ₄) ₂ Mo ₂ O ₇ (aq)	(NH ₄) ₂ SO ₄ (aq) + CuMo ₂ O ₇ (s)
6 ml 2.3 M Cu(NO ₃) ₂ (aq) + 2 ml 0.1 M H ₃ PO ₄ ·12MoO ₃ (aq)	No precipitation

greater HCN filtration capacity. Comparison of Figs. 1(c) and Fig. 3(b) and (c) indicates that sample N1 has the smallest grain-size impregnant, and presumably the best impregnant distribution, of these samples by the fact that it does not have intense, well defined impregnant-related diffraction peaks in its XRD spectrum. Data of good impregnant distribution was presented for sample W5 in Figs. 3(a) and 4(b) and (d). Fig. 5 shows that this sample has better HCN filtration capacity than samples W3 and W4, even though it has much lower Cu²⁺ impregnant loading (as is shown in Table 1). In Fig. 4(f) and (h) EDX data was presented showing that the Cu and Mo impregnant were in intimate contact on the AC substrate. The importance of this intimate contact is reflected in the even HCN and NCCN breakthrough time ratios observed for sample W5.

Off-carbon experiments were performed in order to better understand how the choice of impregnating materials affected impregnant distribution. Aqueous Cu(NO₃)₂, CuSO₄, Na₂MoO₄, (NH₄)₂Mo₂O₇ and H₃PO₄·12MoO₃ solutions were prepared for this study. These solutions were combined in various combinations and visual observations were made. Table 2 lists reactants and their proposed products for solutions studied in this experiment.

The results listed in Table 2 demonstrate that combining aqueous Cu(NO₃)₂ or CuSO₄ with aqueous Na₂MoO₄ or (NH₄)₂Mo₂O₇ results in a precipitation reaction. These results help to explain the relatively poor impregnant distribution for IAC samples W3 and W4 (shown in Figs. 3(c) and (b) and 4(a) and (c)). The poor impregnant distribution and presence of unwanted impregnants (such as NaNO₃ or Na₂SO₄) on the AC substrate after drying can also help to explain the poor HCN filtration capacity of IAC samples W3 and W4. Aqueous Cu(NO₃)₂ and H₃PO₄·12MoO₃ can be combined without precipitation. Further work determined that HNO₃ can be added to this solution without any adverse effects. Impregnating solutions comprised of Cu(NO₃)₂, H₃PO₄·12MoO₃ and HNO₃ have been shown in both on- and off-carbon experiments to be beneficial. The fact that all the impregnating materials can be combined in a single impregnating solution allows the activated carbon substrate to be impregnated in a single step. IAC samples prepared from these solutions have been observed to have good impregnant distribution, as was shown in Figs. 3(a) and 4(b) and (d). The well-dispersed impregnant and beneficial modification of the AC substrate by the HNO₃ treatment resulted in relatively good gas filtration capacity for all challenge gases as can be seen for sample W5 in Fig. 5. These results were achieved at relatively low impregnant loadings. To better understand the useful properties of IAC sample W5, samples W6–W10 (listed in Table 1) were prepared, characterized and tested.

3.3. Copper nitrate, nitric and phosphomolybdic acid based impregnation study.

Samples W9 and W10 were characterized by XRD analysis using a Rigaku Miniflex diffractometer and the results are shown in

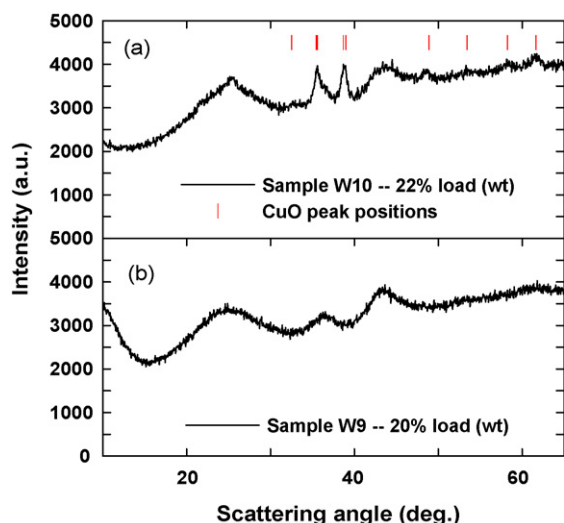


Fig. 6. X-ray diffraction patterns obtained from samples W10 and W9 are shown in panels (a) and (b), respectively.

Fig. 6. For reference, the Bragg peak positions for CuO are indicated. Comparison of these results shows that the diffraction pattern obtained from sample W10 (Fig. 6(a)) exhibits CuO peaks with much greater intensity and definition than those observed in the diffraction pattern of sample W9 (Fig. 6(b)). This is indicative of larger grain-size CuO impregnant on sample W10 as can be inferred from the Scherrer equation [18]. The observation of well defined, intense impregnant-related diffraction peaks, and presumably poor impregnant distribution, was shown in Sections 3.1 and 3.2 to correspond to reduced gas filtration capacity (especially for the HCN challenge gas). Referring to Table 1, the only difference between the two samples is that sample W10 was prepared from an impregnating solution containing 1.2 M HNO₃ and sample W9 was prepared from an impregnating solution with 4 M HNO₃ present. It is reasonable to conclude that the higher HNO₃ concentration in the impregnating solution used to prepare sample W9 was responsible for the improved impregnant distribution.

To further study the impregnant distribution of IAC samples W9 and W10, SEM and EDX analysis was employed. Fig. 7 shows SEM images obtained from these IAC samples at approximately 5000 \times magnification. Panels (a) and (b) show the inner pore structure of samples W9 and W10 respectively. Panels (c) and (d) show EDX pixel maps of the areas shown in panels (a) and (b), respectively. The white pixels represent the presence of copper. Fig. 7(a) shows that the inner surface of sample W9 is relatively clear and does not have any “visual” signs of impregnant. The EDX pixel map showing the Cu distribution of the inner surface of sample W9 (Fig. 7(c)) is indicative of even Cu-impregnant distribution over the carbon surface. The EDX map of the Mo distribution for this area (not shown) also indicated even impregnant distribution. Fig. 7(b) shows an SEM image of the inner surface of sample W10. This image shows a large agglomeration of Cu rich impregnant on the carbon surface, as was confirmed by the EDX pixel map of the Cu-impregnant distribution shown in panel (d). The results obtained from SEM and EDX analysis are consistent with the findings from the XRD analysis presented in Fig. 6, indicating that more concentrated HNO₃ in the aqueous Cu(NO₃)₂, H₃PO₄·12MoO₃ and HNO₃ impregnating solution produces better impregnant distribution on the IAC samples. IAC samples W6–W10 were subjected to dynamic flow testing versus SO₂, NH₃ and HCN challenge gases. Results obtained from these tests are presented in Fig. 8. Sample W8 was tested versus HCN gas only; results for this sample will be discussed later. For comparison, the breakthrough times obtained from testing virgin GC and samples N1 and W5 have been included. Fig. 8 shows that sample W9 exhibits overall gas filtration capacity that is comparable to sample N1. The longer HCN breakthrough time exhibited by the sample N1 is of little consequence because balanced HCN and NCCN breakthrough times are required due to the toxicity of the NCCN gas. When this is considered the HCN and NCCN filtration capacities of samples W9 and N1 are almost equal demonstrating that IAC samples based on the formulation used to prepare sample W9 are promising candidates for use in gas masks capable of filtering a wide variety of irritating and toxic gases!

SO₂ and NH₃ flow test results shown in Fig. 8 indicate that sample N1 has better SO₂ capacity and lower NH₃ capacity than samples W5, W9 and W10. Table 1 shows that these samples have

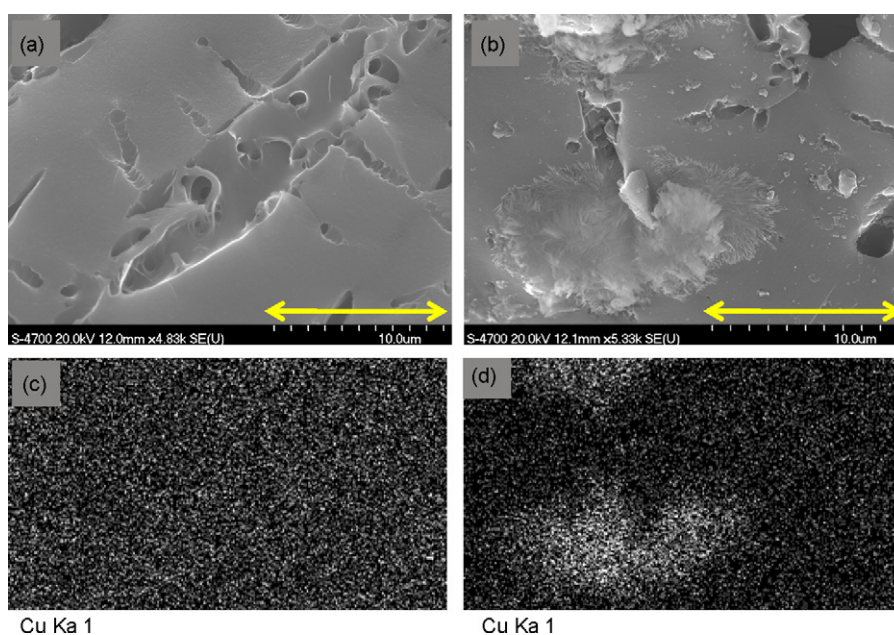


Fig. 7. Panels (a) and (b) show the inner pore structure of samples W9 and W10, respectively. Panels (c) and (d) show EDX pixel maps of the areas shown in panels (a) and (b), respectively. The white pixels represent the presence of copper. The scale bars shown in panels (a) and (b) represent 10 μm.

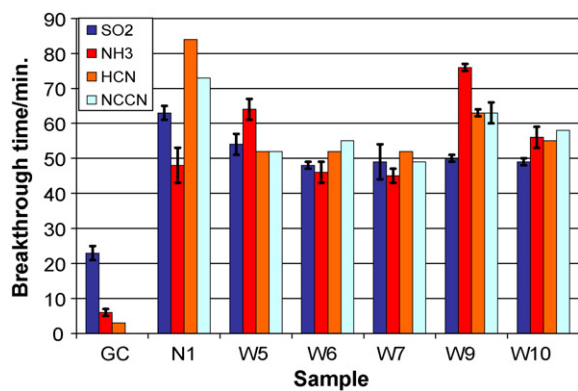


Fig. 8. Dynamic flow test results obtained from challenging samples W6, W7, W9 and W10 with SO₂, NH₃ and HCN challenge gases. For reference the breakthrough times obtained from testing virgin GC and samples N1 and W5 have been included.

been exposed to the most concentrated HNO₃ treatments and these samples probably have higher numbers of acidic surface sites compared to samples W6 and W7. Therefore it is reasonable to correlate the relatively high NH₃ capacity to the acidic nature of these carbons. Comparing the data in Fig. 8 to the impregnating solution contents listed in Table 1, the NH₃ capacity increases as a function of HNO₃ concentration in the parent impregnating solution for these samples. The higher SO₂ capacity shown for sample N1 in Fig. 8 is probably due to the ammoniacal impregnating solution modifying the AC substrate in a manner that gives it a more basic nature. Experimental work to support this statement has not yet been performed.

To investigate the reaction product(s) forming during SO₂ flow tests a soaking study was performed. Approximately 1 g of unexposed IAC and 1 g of SO₂-exposed IAC were taken from sample W9. The IAC samples were placed in a glass jar and covered with approximately 50 ml of distilled water. The jars were sealed and allowed to sit for approximately two days at room temperature. The solution recovered from the vials was poured, through high flow-rate filter paper, into clean glass vials. The recovered solution was placed, uncovered, in an oven and dried at 50 °C until the solution had evaporated. The solids that remained in the vials were removed and subjected to XRD analysis. Small amounts of white powder were obtained from the solution of the unexposed IAC sample. It was not possible to identify these material(s) using XRD analysis. A much larger quantity of light blue powder was recovered from the solution of the SO₂-exposed IAC. The diffraction pattern of this powder is shown in Fig. 9 along with the main Bragg peaks associated with bonnatite (CuSO₄·3H₂O) [17]. The diffraction pattern shown in Fig. 9 is well matched by the CuSO₄·3H₂O peak positions. This shows that CuSO₄ dissolved from the SO₂-exposed IAC (taken from sample W9) during soaking. A proposed reaction mechanism

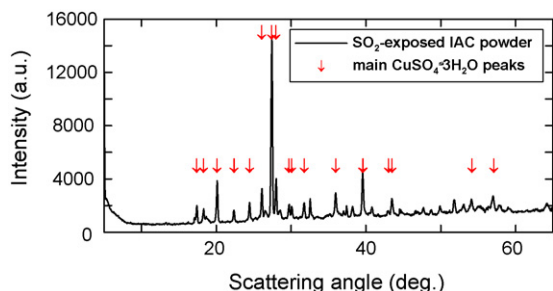


Fig. 9. XRD pattern of powder recovered from solution of SO₂-exposed IAC sample. The main Bragg peak positions for CuSO₄·3H₂O have been indicated for reference.

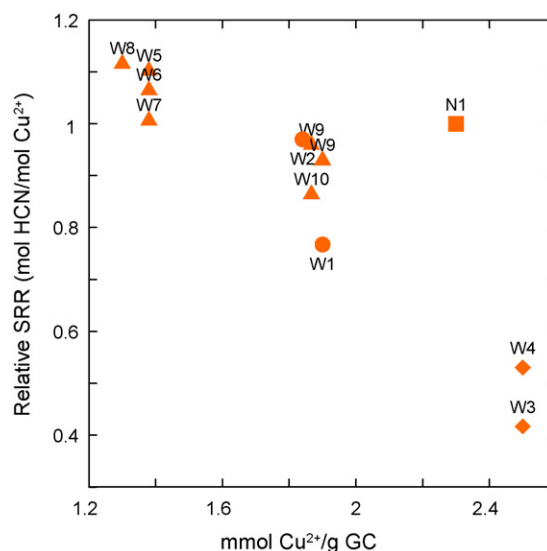


Fig. 10. HCN flow test results obtained from IAC samples N1, W1, W3 and W4–W10. The results are plotted as the Relative SRR (mol HCN/mol Cu²⁺) as a function of Cu-impregnant loading.

can be written as:



Further evidence to support Eq. (2) comes from the fact that drying temperatures used to prepare sample W9 (>190 °C) have been shown in Fig. 6 to be sufficient to convert the Cu(NO₃)₂ impregnant to CuO. CuO is not water soluble, but CuSO₄ is [23]. CuSO₄·3H₂O was only observed in the powder obtained from the soaking experiment performed on SO₂-exposed IAC. It is therefore logical to assume that SO₂ gas and CuO impregnant react to form CuSO₄. This reaction has been written in the literature [7].

The HCN flow test results shown in Fig. 8 demonstrate that the amount of Cu²⁺ impregnant present on the AC substrate plays a critical role in the filtration capacity. Comparison of results obtained from samples W9 and W10, which had approximately the same impregnant loading, show that sample W9 had better HCN capacity. Sample W9 was also shown to have better impregnant distribution in Figs. 6 and 7. To better interpret the role that impregnant distribution plays in gas filtration capacity, the HCN flow test results from all of the IAC samples tested in this study have been plotted as the relative stoichiometric ratio of reaction (SRR) as a function of Cu²⁺ impregnant loading in Fig. 10. The results shown do not take the critical bed amount (CBA) into account when calculating the SRR. The CBA is effectively the amount of the sample bed that does not fully react during the gas exposure and is related to the kinetics of the reaction [11]. To denote that the CBA is not used in our determination of the SRR, we use the designation “relative SRR” in our discussion of these results.

Results shown in Fig. 10 for samples W5–W10 indicate that the concentration of HNO₃ present in the impregnating solution plays an important role in the HCN filtration capacity of the IAC samples. Samples W5–W8 all have approximately the same Cu²⁺ impregnant loading. The concentration of HNO₃ in the impregnating solutions used to prepare these samples decreased in the following order: W5, W8, W6 and W7. Fig. 10 shows that samples with HNO₃ concentration ≥ 4 M in their impregnating solutions had the highest relative SRR values. This same trend is observed for samples W1, W2, W9 and W10 which had higher Cu²⁺ impregnant loadings. From the results shown in Figs. 7, 8 and 11 it is reasonable to state that more concentrated HNO₃ in the impregnating solution results in IAC samples with better impregnant distribution, and this

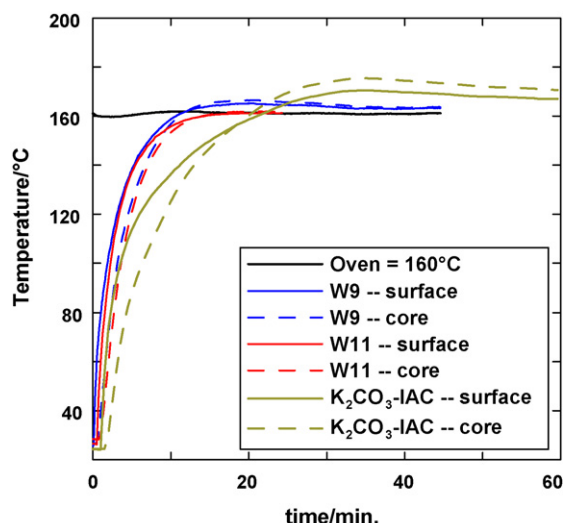


Fig. 11. Results of thermal stability tests at 160 °C performed on samples W9, W11 and the K_2CO_3 -IAC sample.

improved impregnant distribution results in higher HCN filtration efficiency.

Comparison of results for IACs that are shown in Fig. 10 indicate that samples W5–W10 and N1 have comparable relative SRR values. XRD and SEM analysis of these samples showed that they had good impregnant distribution. The effects of poorly distributed impregnant can be observed in the results shown in Fig. 10 for samples W1 and especially samples W3 and W4. Samples W3 and W4 had relative SRR values < 0.6 . Figs. 3(a) and (b) and 4(a) and (c) show that these samples also had relatively poor impregnant distribution. Overall, results obtained from sample characterizations and dynamic flow testing show that good Cu^{2+} impregnant distribution is vital for the IAC samples to have high HCN filtration capacity.

3.4. Thermal stability study

Results discussed in the previous sections showed that IACs produced from aqueous solutions containing $Cu(NO_3)_2$, $H_3PO_4 \cdot 12MoO_3$ and HNO_3 were capable of filtering a wide variety of irritating and toxic gases. These IACs demonstrated filtration capacity versus SO_2 , NH_3 , HCN and NCCN gases that was comparable to samples prepared from ammoniacal solutions [9]. For these IACs to be of commercial interest they must demonstrate thermal stability during shipping and storage.

The thermal stability of samples W9 and W11 were studied. For comparison a commercially available K_2CO_3 -impregnated activated carbon was also studied. The choice of the K_2CO_3 -IAC sample as a standard for comparison was made for two reasons. The first being that it is a commercially available product that is produced, shipped and stored around the world by 3M Canada Company (Brockville, Ontario). If samples W9 and W11 are as thermally stable as the K_2CO_3 -IAC samples, they may be commercially viable from a shipping and storage standpoint. The second reason that this IAC was chosen for comparison is that its thermal properties have been extensively studied and are well understood. Detailed information from these studies is reported in the literature [13,24].

The experimental methods used in the thermal stability tests have been described in the literature [13]. Approximately the same volume of IAC sample was used in all the thermal stability tests. This amount was determined by visual inspection and corresponds to the volume of IAC sample required to fill the cylindrical sample holder. The mass of the different IAC samples studied in this experiment ranged from approximately 13–18 g, due to differences in

the impregnant loading. The temperature of the samples was monitored at the core and on the surface of the cylindrical sample holder and will be clearly distinguished in the reported results. Thermal stability tests were performed over a stable oven temperature range of 100–160 °C in 20 °C increments.

Fig. 11 shows the data obtained from a thermal stability test performed at 160 °C. Data from samples W9, W11 and the K_2CO_3 -IAC samples are shown. The solid line represents the surface temperature measurement and the dashed lines represent the core temperature measurement. Fig. 11 shows that all of the IAC samples were thermally stable at 160 °C oven temperatures. The slightly higher temperatures shown for the K_2CO_3 -IAC sample was due to a 165 °C stable oven temperature being used in that particular test. The results shown here indicate that samples W9 and W11 are as thermally stable as the commercially available K_2CO_3 -IAC samples.

4. Conclusions

Performing on- and off-carbon experiments allowed several important observations to be made. This led to the development of IAC samples that can be prepared from aqueous solutions in a simple and efficient manner. These types of IACs are advantageous because they do not require the use of ammonia or ammonium salts during their preparation. IAC samples prepared from aqueous $Cu(NO_3)_2$, $H_3PO_4 \cdot 12MoO_3$ and HNO_3 containing solutions, with appropriate heat treatments, had gas filtration capacities that were comparable to samples prepared from ammoniacal solutions when challenged with SO_2 , NH_3 and HCN gases.

Using XRD, SEM and EDX analysis it was observed that the use of HNO_3 in aqueous $Cu(NO_3)_2$ -based impregnating solutions improved impregnant distribution on the AC substrate. The improved impregnant distribution was found to result in increased gas filtration capacities, especially for HCN challenge gas. It was found that IAC samples prepared from impregnating solutions with higher HNO_3 concentrations had better impregnant distribution and consequently higher gas filtration capacities. Samples prepared on AC that had been treated with HNO_3 were found to have greatly enhanced NH_3 filtration capacity, which was attributed to the presence of acidic groups on the AC surface. Using SEM and EDX analysis it was observed that intimate contact between the Cu and Mo-impregnant species on the AC substrate results in IAC samples with well balanced NCCN:HCN breakthrough time ratios.

IAC samples prepared from aqueous solutions were found to be as thermally stable as commercially available K_2CO_3 -IAC samples during storage at elevated temperatures. Overall, results reported in this work indicate that IACs prepared from aqueous $Cu(NO_3)_2$, $H_3PO_4 \cdot 12MoO_3$ and HNO_3 containing solutions may be viable candidates for use in broad spectrum respirator applications.

Acknowledgments

The authors would like to thank 3M Canada and NSERC for their financial support. The authors thank Simon Smith and Larry Brey for sharing valuable insight and experience in the field of activated carbon research.

References

- [1] V. Bush, J.B. Conant, W.A. Noyes, Military Problems with Aerosols and Nonpersistent Gases, vol. 1, NRDC Pentagon, Washington DC, 1946, 23–168.
- [2] Y.-W. Lee, H.-J. Kim, J.-W. Park, B.-U. Choi, D.-K. Choi, J.-W. Park, Adsorption and reaction behavior for the simultaneous adsorption of NO–NO₂ and SO₂ on activated carbon impregnated with KOH, Carbon 41 (2003) 1881–1888.
- [3] S.W. Park, H.S. Park, W.K. Lee, H. Moon, Effect of water–vapor on adsorption of methyl-iodide to triethylenediamine-impregnated activated carbons, Sep. Technol. 5 (1995) 35–44.

- [4] C. Petit, C. Karwacki, G. Peterson, T.J. Badosz, Interactions of ammonia with the surface of microporous carbon impregnated with transition metal chlorides, *J. Phys. Chem. C* 111 (2007) 12705–12714.
- [5] H. Fortier, C. Zelenietz, T.R. Dahn, P. Westreich, D.A. Stevens, J.R. Dahn, SO₂ adsorption capacity of K₂CO₃-impregnated activated carbon as a function of K₂CO₃ content loaded by soaking and incipient wetness, *Appl. Surf. Sci.* 253 (2007) 3201–3207.
- [6] H. Fortier, P. Westreich, S. Selig, C. Zeleneitz, J.R. Dahn, Ammonia, Cyclohexane, Nitrogen and water adsorption capacities of an activated carbon impregnated with increasing amounts of ZnCl₂, and designed to chemisorb gaseous NH₃ from an air stream, *J. Colloid Interface Sci.* 320 (2008) 423–435.
- [7] H.-H. Tseng, M.-Y. Wey, Study of SO₂ adsorption and thermal regeneration over activated carbon-supported copper oxide catalysts, *Carbon* 42 (2004) 2269–2278.
- [8] R.E. Wilson, J.C. Whetzel, Impregnated carbon and process of making same, U.S. Patent no. 1519470, 1921.
- [9] D.T. Doughty, W.J. Knebel, J.W. III. Cobes, Chromium-free impregnated activated carbon for adsorption of toxic gases and/or vapours in industrial applications, U.S. Patent no. 5492882, 1996.
- [10] Health Canada, <http://www.hc-sc.gc.ca/ewh-semt/pubs/contaminants/psl2-lsp2/ammonia/index-eng.php> (accessed October 21, 2008).
- [11] H. Fortier, The Science of Impregnation and the Optimization of the Performance of Impregnated Activated Carbons for Gas Masks Applications, Ph.D. Thesis, Department of Chemistry, Dalhousie University, Nova Scotia, Canada, 2007.
- [12] P. Westreich, H. Fortier, S. Flynn, S. Foster, J.R. Dahn, Exclusion of salt solutions from activated carbon pores and relationship to contact angle on graphite, *J. Phys. Chem. C* 111 (2007) 3680–3684.
- [13] H. Fortier, S. Zhang, J.R. Dahn, Simulations of isothermal oven tests of impregnated activated carbons in cylindrical and cubic sample holders, *Carbon* 42 (2004) 2385–2392.
- [14] Omega, <http://www.omega.com/teref/thermcolorcodes.html> (accessed June 26, 2008).
- [15] U.S. Department of Labor, <http://www.osha.gov/SLTC/healthguidelines/hydrogencyanide/recognition.html>, (accessed June 26, 2008).
- [16] B.R. Alves, A.J. Clark, An examination of the products formed on reaction of hydrogen cyanide and cyanogen with copper, chromium (6+) and copper-chromium (6+) impregnated activated carbons, *Carbon* 24 (1986) 287–294.
- [17] International Centre for Diffraction Data, <http://www.icdd.com>, (accessed July 4, 2008).
- [18] H.P. Klug, L.E. Alexander, X-ray Diffraction Procedures: For Polycrystalline and Amorphous Materials, John Wiley & Sons, London, 1974, 687.
- [19] B. Xiao, K.M. Thomas, Adsorption of aqueous metal ions on oxygen and nitrogen functionalized nanoporous activated carbons, *Langmuir* 21 (2005) 3892–3902.
- [20] J.W.H. Smith, P. Westreich, A.J. Smith, H. Fortier, L.M. Croll, J.H. Reynolds, J.R. Dahn, Investigation of copper oxide impregnants prepared from various precursors for respirator carbons, *J. Colloid Interface Sci.* 341 (2010) 162–170.
- [21] C.-C. Huang, H.-S. Li, C.-H. Chen, Effect of surface acidic oxides of activated carbon on adsorption of ammonia, *J. Hazard. Mater.* 159 (2008) 523–527.
- [22] L.A. Brey, S.J. Smith and G.E. Weagle, Broad spectrum filter system including tungsten-based impregnant and being useful for filtering contaminants from air or other gases, U.S. Patent no. 7309513, 2007.
- [23] D.R. Lide, CRC Handbook of Chemistry and Physics, Electronic ed., CRC Press, Boca Raton, 2004, 4–56.
- [24] S. Zhang, S. Stewart, T. Hatchard, J.R. Dahn, Thermal runaway predictions for impregnated activated carbons from isothermal DSC measurements, *Carbon* 41 (2003) 903–913.